Journal of Applied Polymer Science

# Synergistic Effect Between Silicone-Containing Macromolecular Charring Agent and Ammonium Polyphosphate in Flame Retardant Polypropylene

**Xuejun Lai, Changyu Yin, Hongqiang Li, Xingrong Zeng**
College of Materials Science and Engineering, South China University of Technology, Guangzhou 510640, China
Correspondence to: X. Lai (E-mail: xuejun.lai@gmail.com) and X. Zeng (E-mail: psxrzeng@gmail.com)

**ABSTRACT:** A novel silicone-containing macromolecular charring agent (Si-MCA) was synthesized via polycondensation, and it was combined with ammonium polyphosphate (APP) to flame retard polypropylene (PP). The results showed that Si-MCA exhibited a good synergistic effect with APP in flame retardant PP. When the content of APP was 18.7 wt % and Si-MCA was 6.3 wt %, the limiting oxygen index value of the PP/APP/Si-MCA composite was 33.5%, and the vertical burning (UL 94) test classed a V-0 rating. The peak heat release rate, total heat release, average mass loss rate, and total smoke production of the composite were also decreased significantly. Moreover, the PP/APP/Si-MCA composite showed an outstanding water resistance. After soaking in 70°C water for 168 h, the PP/APP/Si-MCA composite could still reach a UL 94 V-0 rating at 20.0 wt % IFR loading, whereas the PP/APP/PER composite failed to pass the UL 94 test even at 25.0 wt % IFR loading. Thermogravimetric analysis, thermogravimetry-Fourier transform infrared spectrometry, and scanning electron microscopy-energy dispersive X-ray spectrometry results revealed that a compact and thermostable intumescent char was formed by APP/Si-MCA during burning, thus effectively improved the flame retardancy of PP. The possible synergistic mechanism between APP and Si-MCA was also discussed. © 2014 Wiley Periodicals, Inc. J. Appl. Polym. Sci. **2015**, *132*, 41580.

**KEYWORDS:** composites; flame retardance; polyolefins; thermogravimetric analysis

Received 3 July 2014; accepted 1 October 2014
**DOI: 10.1002/app.41580**

## INTRODUCTION

In recent years, intumescent flame retardants (IFRs) have attracted more and more attention in flame retardant polypropylene (PP), due to their being halogen-free, environmental-friendly, antidripping, and low smoke. Generally, an IFR system is composed of three ingredients, including a charring agent, an acid catalyst, and a blowing agent. The most widely used IFR is ammonium polyphosphate/pentaerythritol/melamine (APP/PER).[1,2] When being burned, it generates a multicellular swollen char on the surface of polymer, slowing down the heat and mass transfer, thus protects the substrate from burning.[3] However, the charring agent PER is a small-molecule compound containing four hydroxyls, which is water-soluble and has poor compatibility with the polymer matrix.[4–6] As a result, the flame retardant in the composites is easily attacked by water and exuded, leading to a deterioration of the flame retardancy.

To overcome the shortcoming, macromolecular charring agents possessing low water solubility and good charring capability, such as polyamide,[7–10] caged bicyclic phosphates,[11–13] triazine derivatives,[14–19] and so on were used to replace PER. Recently, triazine derivatives have aroused a great deal of attention due to their little water solubility and outstanding charring performance. They can act as efficient charring agents because they contain thermostable triazine rings and can form char easily during combustion.[15,20] In our previous work,[21] a triazine-based macromolecule (TBM) was synthesized via solution polycondensation of cyanuric chloride (CNC), ethanolamine, and diethylenetriamine. TBM possessed little water solubility and superior char-forming capability, and it showed a good synergism with melamine pyrophosphate (MPP) in flame retardant PP. Unfortunately, to achieve a UL 94 rating, more than 25.0 wt % MPP/TBM was needed, which increased the cost and deteriorated the mechanical properties of the PP/IFR composites. Some research works[22–26] indicated that silicone-containing compounds could effectively improve the flame-retardant efficiency of the PP/IFR composites. Chen and Jiao[23] used hydroxyl silicone oil (HSO) and IFR to flame-retard PP and found that a small amount of HSO could significantly enhance the quality of the swollen char, thus improved the flame retardancy of the PP/IFR composites. Therefore, the combination of siloxane and triazine ring in a macromolecule proposed here is considered to be a promising way to prepare efficient charring agent.

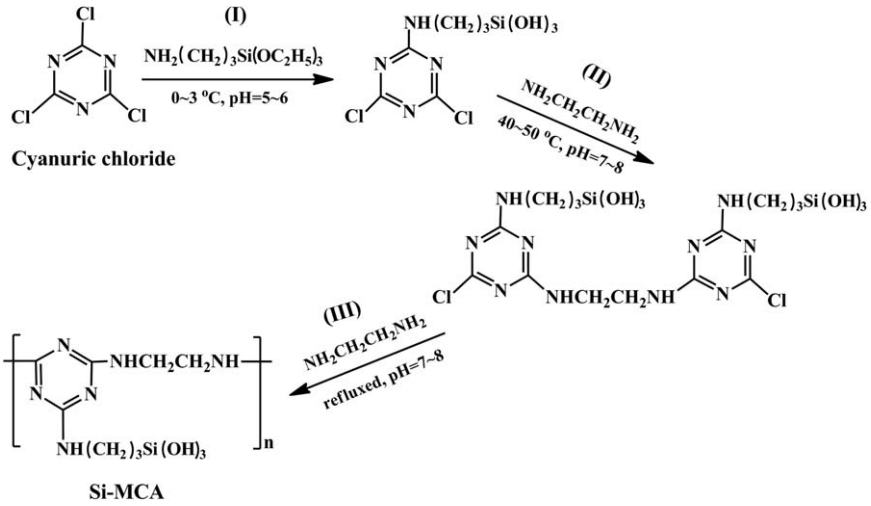


**Scheme 1.** Synthetic route of Si-MCA.

In this work, a novel silicone-containing macromolecular charring agent (Si-MCA) was synthesized via the polycondensation of CNC, ethylenediamine, γ-aminopropyl triethoxysilane, and it was combined with APP to flame retard PP. The chemical structure of Si-MCA was characterized by Fourier transform infrared spectroscopy (FTIR) and solid-state $^{13}C$ nuclear magnetic resonance ($^{13}C$-NMR). The synergistic effect between Si-MCA and APP on the flame retardancy and thermal properties of PP were investigated by limiting oxygen index (LOI), vertical burning test (UL 94), cone calorimetric test (CCT), thermogravimetric analysis (TGA), thermogravimetry-Fourier transform infrared spectrometry (TG-FTIR), and scanning electron microscopy-energy dispersive X-ray spectrometry (SEM-EDXS). The possible synergistic mechanism between Si-MCA and APP was also explored.

## EXPERIMENTAL

### Materials

CNC was provided by Yingkou Sanzheng Organic Chemical Industry, China. Ethanediamine was obtained from Shanghai Lingfeng Chemical Reagents, China. γ-Aminopropyl triethoxysilane (A-1100) was purchased from Union Carbide Corporation. PP (T30S), a granulated product with a melt flow index of 3.0 g/10 min (230°C, 2.16 kg), was supplied by Maoming Petrochemical, China. APP, polymerization degree > 1500, water solubility at 70°C: 2.5 g/100 mL $H_2O$) was obtained from Jiangmen Topchem Technology, China. PER water solubility at 70°C: 15.0 g/100 mL $H_2O$) was purchased from Tianjin Kermel Chemical Reagent, China. Antioxidant (IRGANOX B215) was provided by Ciba Specialty Chemicals, Switzerland. All these commercial materials were used directly without further purification.

### Synthesis of Si-MCA

500 mL acetone and 0.4 mol CNC were added in a 1000 mL round bottom flask, and stirred at 0–5°C until a transparent solution was formed. 0.4 mol γ-aminopropyl triethoxysilane (A-1100) was dissolved in another 50 mL acetone. The mixture and NaOH aqueous solution were added dropwise into the CNC solution. The pH of the solution was kept at 5–6. The reaction lasted for 4 h at 0–5°C.

Subsequently, the reaction temperature was heated up to 40–50°C. A water solution containing 0.2 mol ethanediamine and 0.5 mol NaOH was added dropwise into the flask (the pH was kept at 7–8). The reaction lasted for another 4 h. Then, the solution was filtrated and washed with acetone and alcohol for several times. After dried at 90°C under vacuum for 6 h, the intermediate (product I) was obtained.

Finally, 500 mL dioxane and the product I were added in a 1000 mL round bottom flask and stirred at 95–100°C until a homogeneous mixture was formed. Another water solution containing 0.2 mol ethanediamine and 0.5 mol NaOH was added dropwise into the flask (the pH was also kept at 7–8), and the reaction was kept under reflux for 6 h. It was then washed with a large excess of hot acetone and alcohol. After dried at 100°C under vacuum, the silicone-containing macromolecule charring agent (Si-MCA) was obtained (yield: 85.3%). The degree of polymerization for Si-MCA was about 48 (number-average molecular weight was 13,000). The elemental content of C, N, O, Si, and H were 37.2 wt %, 30.5 wt %, 16.8 wt %, 10.8 wt %, and 4.7 wt %, which were approximately in accordant with their theoretical value, respectively. The water solubility of Si-MCA at 70°C was 0.9 g/100 mL. The synthetic route of Si-MCA was shown in Scheme 1.

### Preparation of Flame Retardant PP

PP, APP, Si-MCA, and PER were dried in a vacuum oven at 100°C for 6 h before use. Then PP, APP, Si-MCA, and PER were melt-mixed on a two-roll mill (XK-160, Changzhou Shuangfeng Machinery Factory, China) at 170°C for 15 min. The prepared composites were molded under compression (15 MPa) at 180°C for 6 min and cooled to room temperature naturally to obtain flame retardant PP sheets with standard size for further testing. The formulations of the flame retardant PP are listed in Table I.

### Characterization and Measurement

**FTIR.** The samples were mixed with KBr powder, and the mixture was pressed into a tablet. The FTIR spectra of the samples

**Table I.** Mechanical Properties of the PP/IFR Composites with Different Formulation

| Sample | Composition of PP/IFR | | | | Tensile strength (MPa) | Impact strength (kJ/m$^2$) |
|---|---|---|---|---|---|---|
| | PP (wt %) | APP (wt %) | Si-MCA (wt %) | PER (wt %) | | |
| PP | 100 | 0 | 0 | 0 | 35.0 ± 1.0 | 3.0 ± 0.2 |
| PP-1 | 75.0 | 25.0 | 0 | 0 | 25.6 ± 0.5 | 2.7 ± 0.2 |
| PP-2 | 75.0 | 0 | 0 | 25.0 | 20.5 ± 1.2 | 2.2 ± 0.3 |
| PP-3 | 75.0 | 0 | 25.0 | 0 | 29.0 ± 0.8 | 3.2 ± 0.2 |
| PP-4 | 75.0 | 18.7 | 6.3 | 0 | 27.4 ± 0.7 | 3.1 ± 0.2 |
| PP-5 | 75.0 | 18.7 | 0 | 6.3 | 23.9 ± 0.8 | 2.5 ± 0.3 |
| PP-6 | 80.0 | 15.0 | 5.0 | 0 | 30.5 ± 0.5 | 3.3 ± 0.2 |
| PP-7 | 80.0 | 15.0 | 0 | 5.0 | 26.1 ± 1.0 | 2.8 ± 0.5 |

were recorded by using a Tensor 27 spectrometer (Bruker Optics, Germany), at a resolution of 4 cm$^{-1}$. The measurements were carried out in the region of 4000–400 cm$^{-1}$.

**Solid-State $^{13}$C-NMR.** The $^{13}$C-NMR spectrum of the sample was recorded on an AVANCE AV-400 Fourier transform superconducting magnetic resonance spectrometer (Bruker, Germany).

**TGA.** The TGA was carried out by using a thermogravimeter (TG209, Netzsch Instruments, Germany) from 30°C to 700°C at a linear heating rate of 20°C/min under an air flow of 30 mL/min. Each sample was measured in an alumina crucible with a weight about 10 mg.

**TG-FTIR.** The TG-FTIR instrument consists of a thermogravimeter (TG209, Netzsch Instruments, Germany), a Fourier transform infrared spectrometer (Tensor 27, Bruker Optics, Germany), and a transfer tube with an inner diameter of 1 mm connecting the TG and the infrared cell. The investigation was carried out from 30°C to 750°C at a linear heating rate of 20°C/min under a nitrogen flow of 30 mL/min. To reduce the possibility of pyrolysis gas condensing along the transfer tube, the temperature of the infrared cell and transfer tube were set to 230°C.

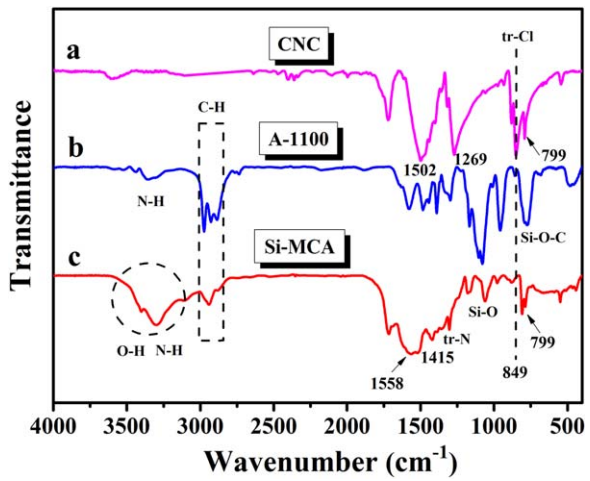


**Figure 1.** FTIR spectra of CNC, A-1100, and Si-MCA. [Color figure can be viewed in the online issue, which is available at wileyonlinelibrary.com.]

**LOI.** The LOI test was conducted by using an oxygen index instrument (HC-2, Jiangning Analysis Instrument, China) according to ASTM D 2863-2008. The dimensions of the specimens were 80 mm × 10 mm × 4 mm.

**Vertical Burning (UL 94) Test.** The vertical burning (UL 94) test was conducted on a vertical burn instrument (CFZ-3, Jiangning Analysis Instrument, China) according to ANSI/UL 94–2010. The dimensions of the specimens were 127 mm × 12.7 mm × 3.2 mm.

**Water-Resistance Test.** The samples were put in distilled water at 70°C and kept at this temperature for 168 h. The treated samples were subsequently taken out and dried in a vacuum oven at 70°C to constant weight. The water resistance of the composites was evaluated by the change of LOI values and UL 94 rating after the water treatment. All the samples were operated for five times and the average value was recorded.

**CCT.** The CCT was carried out by using a cone calorimeter (Fire Testing Technology, UK) according to ISO5660. Each specimen, with a dimension of 100 mm × 100 mm × 4 mm, was wrapped in aluminium foil and exposed horizontally to an external heat flux of 35 kW/m$^2$. All the samples were run in duplicate, and the average value was recorded. The residues of

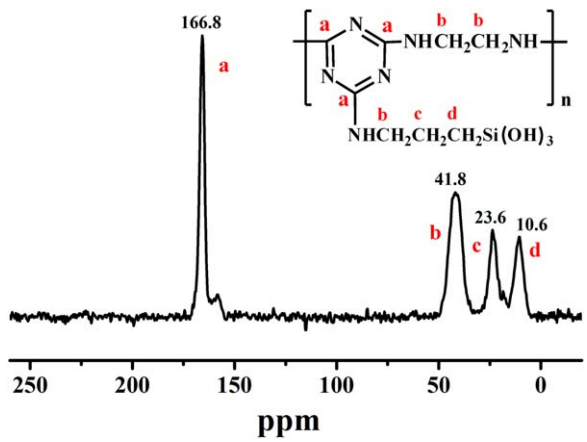


**Figure 2.** Solid-state $^{13}$C-NMR spectrum of Si-MCA. [Color figure can be viewed in the online issue, which is available at wileyonlinelibrary.com.]

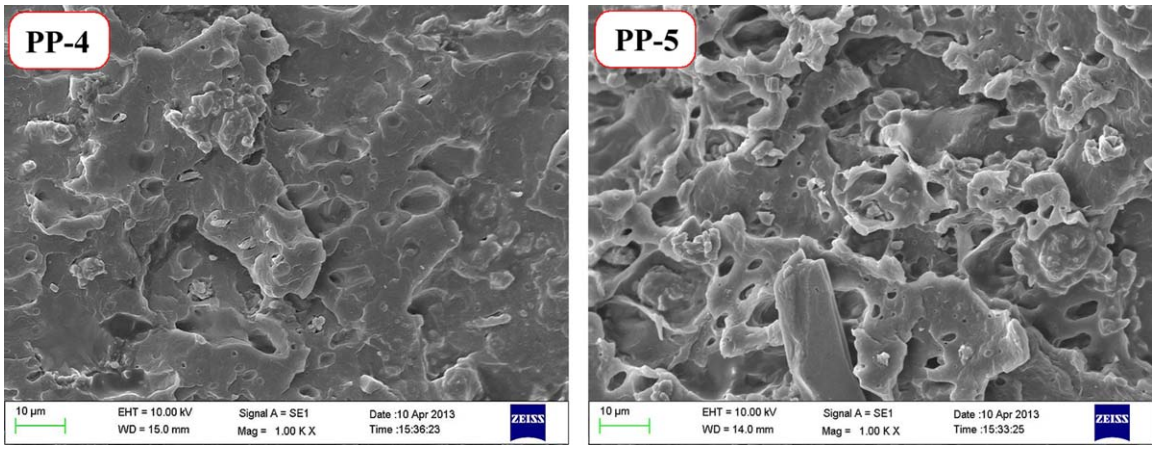


**Figure 3.** SEM images of the fractured surface of PP-4 and PP-5. [Color figure can be viewed in the online issue, which is available at wileyonlinelibrary.com.]

the samples after the CCT were photographed by a digital camera (PowerShot A2000 IS, Canon, Japan).

**SEM-EDXS.** The morphology of the specimens was observed by a SEM (EV0–18, Carl Zeiss Jena, Germany) with an accelerating voltage of 10.0 kV. The composites were cryogenically fractured in liquid nitrogen and then coated with a conductive gold layer before observation. EDXS results of the upper surfaces of residue char for the flame retardant PP were measured by an EDXS.

## RESULTS AND DISCUSSION

### FTIR and Solid-State $^{13}$C-NMR Spectra of Si-MCA

Figure 1 shows the FTIR spectra of CNC, A-1100, and Si-MCA. For CNC, the main characteristic peaks were listed as follows: 1502 $cm^{-1}$ ($\nu_{-N=C-}$), 1269 $cm^{-1}$ ($\nu_{C-N}$), 849 $cm^{-1}$ ($\nu_{tr-Cl}$, tr meant triazine ring here), and 799 $cm^{-1}$ ($\nu_{tr}$).[15] A-1100 was mainly characterized by the following peaks: 3300 $cm^{-1}$ ($\nu_{N-H}$), 2972 and 2886 $cm^{-1}$ ($\nu_{C-H}$ of $-CH_3$), 2928 $cm^{-1}$ ($\nu_{C-H}$ of $-CH_2-$), 1079 $cm^{-1}$ ($\nu_{Si-O}$), 792 $cm^{-1}$ ($\nu_{Si-O-C}$). As shown in Figure 1(c), after CNC reacted with A-1100 and ethanediamine, the bands ascribed to the $\nu_{tr-Cl}$ (849 $cm^{-1}$) disappeared, while a new peak appeared at 1332 $cm^{-1}$ ($\nu_{tr-N}$), indicating that the Cl atoms attached on the triazine rings were totally replaced by the N atoms of the $\gamma$-aminopropyl triethoxysilane and the ethanolamine. Besides, the appearance of the characteristic peaks of triazine ring, A-1100 and ethanediamine in Figure 1(c) further confirmed that Si-MCA was successfully synthesized.

Figure 2 shows the solid-state $^{13}$C-NMR spectrum of Si-MCA. The signal at a chemical shift of 166.8 ppm was assigned to the C atoms of the triazine ring.[16,17] The peak at 41.8 ppm was ascribed to the C atom of $-NH-CH_2-$ group. The characteristic signals located at 23.6 and 10.6 ppm were attributed to the C atoms of and $-CH_2-\underline{C}H_2-CH_2-$ and $-Si-CH_2-$ groups, respectively. Combined with the FTIR analysis, it could be concluded that Si-MCA was successfully synthesized.

### Mechanical Properties of Flame Retardant PP

Table I lists the mechanical properties of the PP/IFR composites with different formulation. The tensile and impact strengths of pure PP were 35.0 ± 1.0 MPa and 3.0 ± 0.2 kJ/m$^2$, respectively. For PP-1 and PP-2, when 25 wt % of APP (or PER) was incorporated into the PP matrix, the mechanical properties of the composites were severely deteriorated due to the poor compatibility between APP (or PER) and PP, while Si-MCA had less negative effect on the mechanical properties of PP. When using the same amount of IFR, the PP/APP/Si-MCA composites showed better mechanical properties in comparison with the PP/APP/PER composites. The tensile and impact strengths of PP-4 were 27.4 ± 0.7 MPa and 3.1 ± 0.2 kJ/m$^2$, which were about 14.6% and 24.0% higher than those of PP-5, respectively. This could be explained by the following reasons: on the one hand, Si-MCA was a macromolecular compound and had lower polarity than PER; on the other hand, Si-MCA could act as a coupling agent, whose Si—OH groups could interact with the —OH, $-NH_4$, and —P=O groups of APP, resulting in the improvement of the compatibility between APP and the polymer matrix. This could be verified by the SEM images of the fracture surface of PP-4 and PP-5, as shown in Figure 3. For PP-5, the flame retardant particles were irregularly distributed on the surface of the polymer matrix and formed some big agglomerates. Many microgaps were observed between the particles and the matrix. In contrast, the flame retardants were

**Table II.** LOI and UL-94 Results of the Samples Before and After Water Soaking (70°C, 168 h)

| | Before soaking | | After soaking | |
|---|---|---|---|---|
| Sample | LOI (%) | UL-94 | LOI (%) | UL-94 |
| PP | 17.5 ± 0.2 | Failed | 17.5 ± 0.2 | Failed |
| PP-1 | 26.0 ± 0.3 | Failed | 24.0 ± 0.2 | Failed |
| PP-2 | 21.5 ± 0.2 | Failed | 18.5 ± 0.2 | Failed |
| PP-3 | 24.5 ± 0.2 | Failed | 23.5 ± 0.3 | Failed |
| PP-4 | 33.5 ± 0.5 | V-0 | 30.0 ± 0.2 | V-0 |
| PP-5 | 31.0 ± 0.2 | V-0 | 26.5 ± 0.2 | Failed |
| PP-6 | 30.5 ± 0.5 | V-0 | 28.5 ± 0.5 | V-0 |
| PP-7 | 27.5 ± 0.2 | V-2 | 24.0 ± 0.5 | Failed |

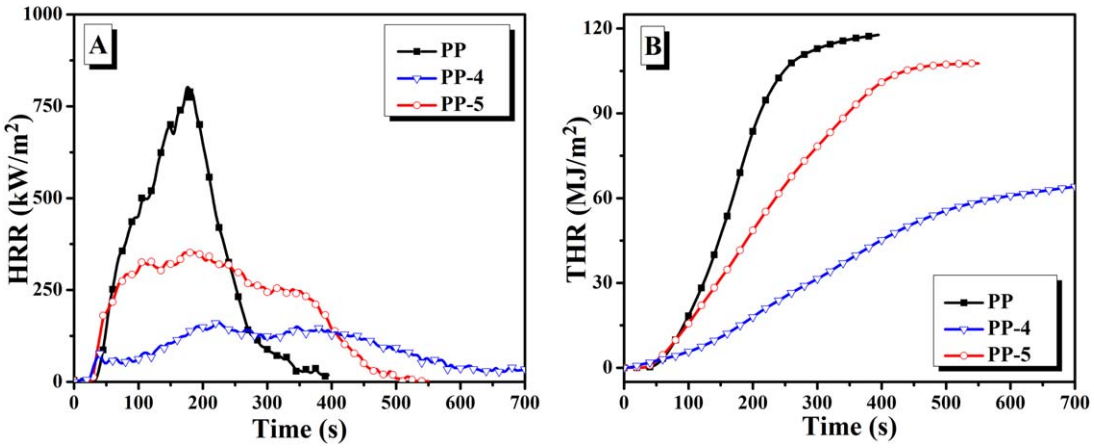


**Figure 4.** HRR (A) and THR (B) curves of PP and flame retardant PP. [Color figure can be viewed in the online issue, which is available at wileyonlinelibrary.com.]

dispersed more uniformly on the surface of PP-4, and the interface between the flame retardant particles and the matrix became vaguer, indicating that the compatibility between these two phases was improved.

### Flame Retardancy and Water Resistance of the Flame Retardant PP

Table II presents the LOI and UL 94 results of the flame retardant PP before and after water soaking. It could be seen that APP, PER, and Si-MCA used alone showed low flame retardancy. The LOI value of PP-1 containing 25.0 wt % APP was only (26.0 ± 0.3)%, and the UL 94 test classed no rating. When using 6.3 wt % PER to replace the same amount of APP, the LOI value of the flame retardant PP (PP-5) was increased from (26.0 ± 0.3)% to (31.0 ± 0.2)%, and the UL 94 result was improved from no rating to V-0 rating. However, after soaking in 70°C water for 168 h, the LOI of PP-5 was decreased to (26.5 ± 0.2)%, and its UL 94 result was degraded to no rating. When incorporating the same amount of IFR into PP, the LOI values of the PP/APP/Si-MCA composites were higher than those of PP/APP/PER, indicating that Si-MCA showed a better synergistic effect with APP in flame retardant PP. When the content of APP was 15.0 wt % and Si-MCA was 5.0 wt %, the LOI value of the composite (PP-6) was (30.5 ± 0.5)% and classed a UL 94 V-0 rating, while the LOI value of PP-7 was (27.5 ± 0.2)% and classed a UL 94 V-2 rating. Moreover, it is worth noting that after water soaking, PP-6 could still achieve a V-0 rating at 20.0 wt % IFR loading, whereas the PP-5 failed to pass the UL 94 test even at 25.0 wt % IFR loading. These might be attributed to the lower water solubility of Si-MCA and its better compatibility with the polymer matrix.

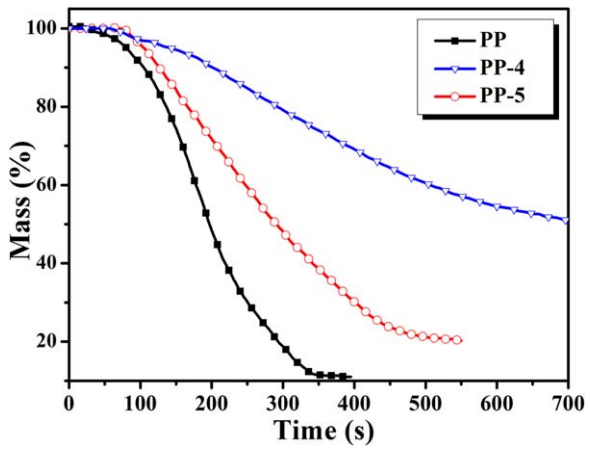


**Figure 5.** Mass lose curves of PP and flame retardant PP. [Color figure can be viewed in the online issue, which is available at wileyonlinelibrary.com.]

### CCT

Figures 4 and 5 show the heat release rate (HRR), total heat release (THR) curves, and mass loss curves of PP and flame retardant PP, and their characteristic parameters are listed in Table III. The pure PP was burnt fiercely after ignition and achieved a peak heat release rate (pHRR) of 815 ± 41 kW/m$^2$ at 175 ± 5 s, and it was burnt out within 390 ± 5 s. With the incorporation of APP/PER and APP/Si-MCA, the pHRR, THR, average mass loss rate (av-MLR), peak smoke production rate (pSPR), and total smoke production (TSP) of the composites were significantly decreased, and the combustion time of the composites was greatly prolonged in comparison with the pure PP, which was attributed to the formation of the intumescent protective char. For PP-4, the pHRR, THR, av-MLR, and TSP were 164 ± 23 kW/m$^2$, 72 ± 11 MJ/m$^2$, 0.02 ± 0.01 g/s m$^2$, and 10 ± 2 m$^2$, which were about 53.7%, 33.3%, 66.7%, and 41.2% lower than those of PP-5, respectively. However, the time to ignition (TTI) was decreased with the addition of APP/PER and APP/Si-MCA. The TTIs of PP, PP-4, and PP-5 were 35 ± 2 s, 27 ± 1 s, and 30 ± 2 s, respectively. This could be explained by that the temperature of the composite surfaces was increased more quickly because the presence of a solid-like intumescent layer effectively prevented the heat transfer.[21] It should be noted that the HRR and THR curves of PP-4 were much flatter than that of PP-5 during the combustion, indicating the former burnt more slowly and gently than the latter. At the end of the CCT, the residue of PP-4 as high as 50.4 ± 6.5 wt %, whereas the residue left by PP-5 was only 20.2 ± 3.3 wt %, which suggested that PP-4 had much better charring performance and the

**Table III.** Characteristic Parameters of the CCT PP and Flame Retardant PP

| Sample | TTI (s) | pHRR (kW/m$^2$) | av-HRR (kW/m$^2$) | THR (MJ/m$^2$) | av-MLR (g/s·m$^2$) | pSPR (m$^2$/s) | TSP (m$^2$) | Residue (%) |
|---|---|---|---|---|---|---|---|---|
| PP | 35 ± 2 | 815 ± 41 | 280 ± 10 | 119 ± 6 | 0.09 ± 0.02 | 0.09 ± 0.01 | 14 ± 3 | 0 |
| PP-4 | 27 ± 1 | 164 ± 23 | 77 ± 3 | 72 ± 11 | 0.02 ± 0.01 | 0.03 ± 0.01 | 10 ± 2 | 50.4 ± 6.5 |
| PP-5 | 30 ± 2 | 354 ± 36 | 209 ± 8 | 108 ± 13 | 0.06 ± 0.02 | 0.07 ± 0.01 | 17 ± 2 | 20.2 ± 3.3 |

formed char could effectively protect the substrate material from burning.

**Morphology and SEM-EDXS Analysis of the Residue Char**

Figure 6 shows the digital photographs and SEM images of the residue char for PP-4 and PP-5 after CCT. For PP-4, it could be clearly seen that a compact and continuous intumescent char was formed and covered on the substrate [Figure 6(a)], which could effectively prevent both heat and combustible gases transfer. This was also confirmed by the SEM-EDXS. As shown in Figure 6(a′), the surface of char layer for PP-4 was dense and compact, and its chemical compositions included 32.4 wt % carbon (C), 10.4 wt % nitrogen (N), 43.2 wt % oxygen (O), 11.6 wt % phosphorus (P), and 2.4 wt % silicon (Si). The high

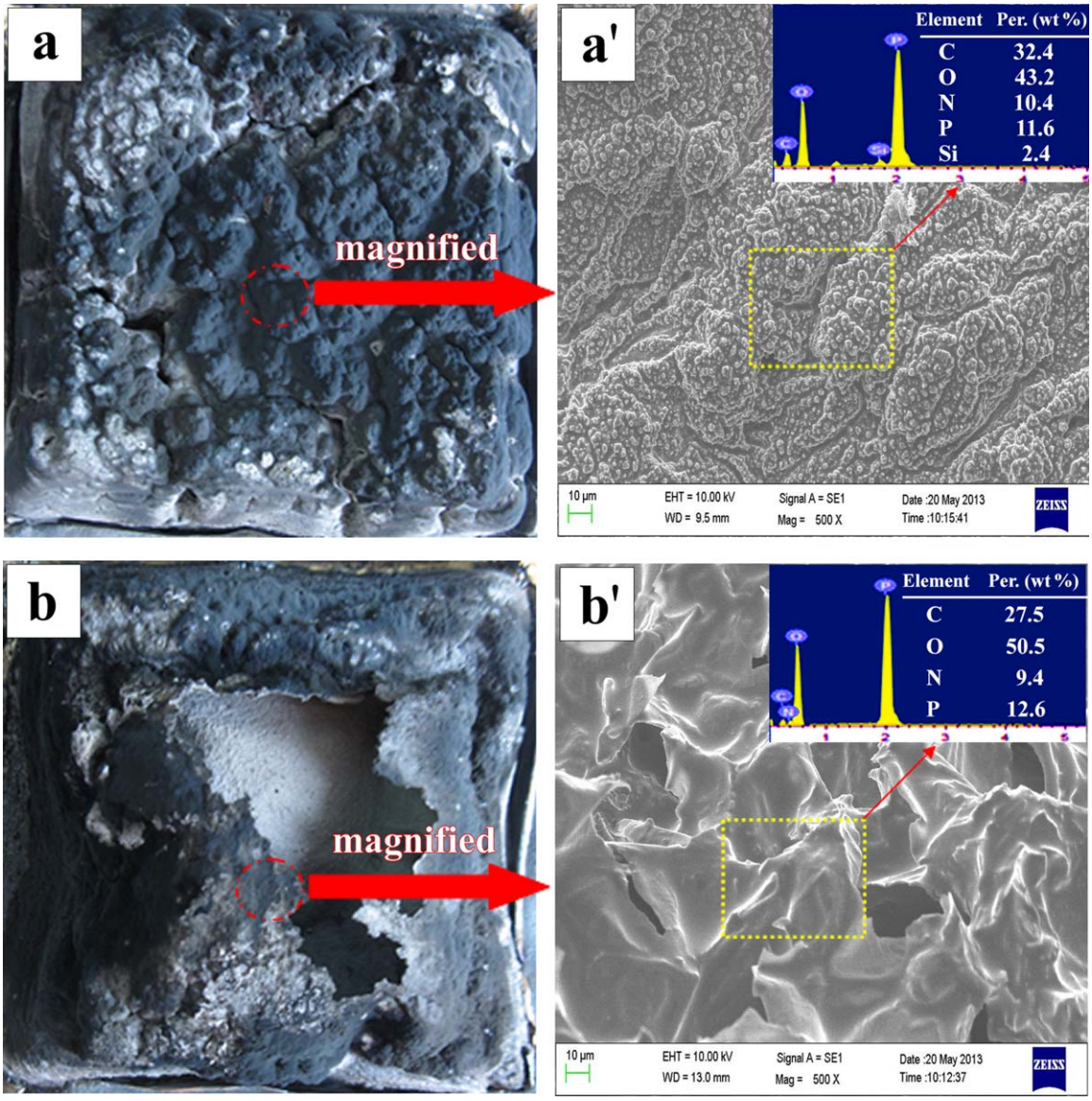


**Figure 6.** Digital photographs, SEM images, and chemical compositions of the residue char for PP-4 and PP-5 after CCT. [Color figure can be viewed in the online issue, which is available at wileyonlinelibrary.com.]

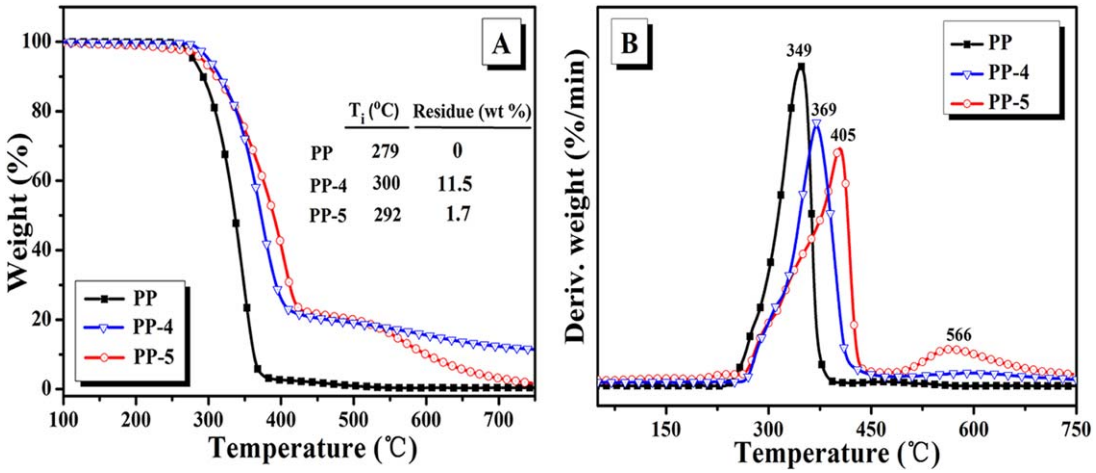


**Figure 7.** TGA (A) and DTG (B) curves of PP and flame retardant PP. [Color figure can be viewed in the online issue, which is available at wileyonlinelibrary.com.]

C, P, and Si contents of the residue suggested that the C atoms were probably crosslinked with the P and Si atoms to form a thermostable char.[11] In contrast, the char layer of PP-5 was relatively thin and easily broken up, which could not effectively prevent either heat or combustible gases transfer during the combustion, resulting in the unsatisfactory flame retardancy of the composite. This could be further verified in Figure 6(b′). Some cracks and cavities were observed on the char layer of PP-5, and the residue was mainly composed of C and O atoms, which probably explained why the char layer was low efficient and thermal instable at the high temperature.

### Thermal Behavior and TG-FTIR Analysis

Figure 7 shows the TGA and DTG curves of PP and flame retardant PP. The pure PP decomposed rapidly from 279 to 380°C, and left no residue at 750°C. The initial decomposition temperature ($T_i$, was defined as the temperature at which 5% mass loss occurred) and the maximum decomposition temperature ($T_{max}$) of PP-5 were 292°C and 405°C, which were 13°C and 56°C higher than those of PP, respectively. This was mainly attributed to the formation of the intumescent char, which protected the substrate material from decomposing. However, the residue char was thermal instable because a mass loss around 566°C was distinctly observed, and the residue left at 750°C was only 1.7 wt %. For PP-4, the $T_i$ and $T_{max}$ were 21°C and 20°C higher than those of PP, and its residue at 750°C was as high as 11.5 wt %. The results indicated that APP/Si-MCA had better charring performance than APP/PER, and the char layer formed by PP-4 was more thermostable at the high temperature.

The interaction between APP and Si-MCA could be revealed by comparing their experimental and calculated TGA results. Figure 8 shows the experimental and calculated TGA curves of APP/Si-MCA. The experimental one was directly obtained from the thermogravimeter, while the calculated one was the sum of the normalized weight losses of APP and Si-MCA. The distinct difference between the experimental and calculated results indicated a strong interaction between APP and Si-MCA. Below

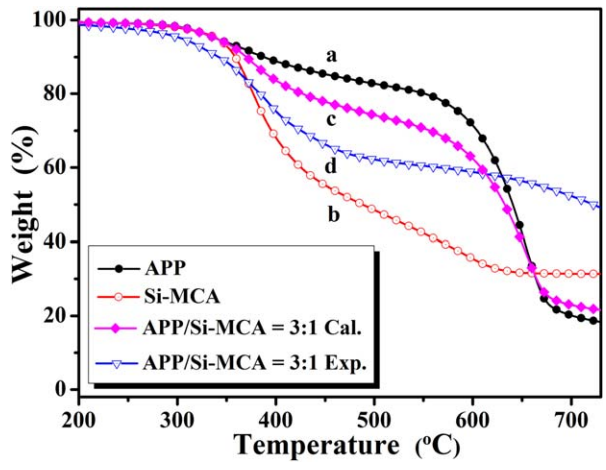


**Figure 8.** Experimental and calculated TGA curves of APP/Si-MCA. [Color figure can be viewed in the online issue, which is available at wileyonlinelibrary.com.]

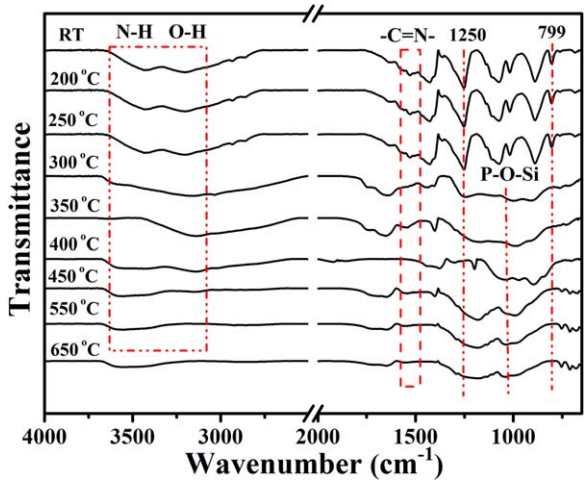


**Figure 9.** FTIR spectra of APP/Si-MCA after heat treatment at different temperature for 15 min. The mass ratio of APP to Si-MCA was 3 : 1. [Color figure can be viewed in the online issue, which is available at wileyonlinelibrary.com.]

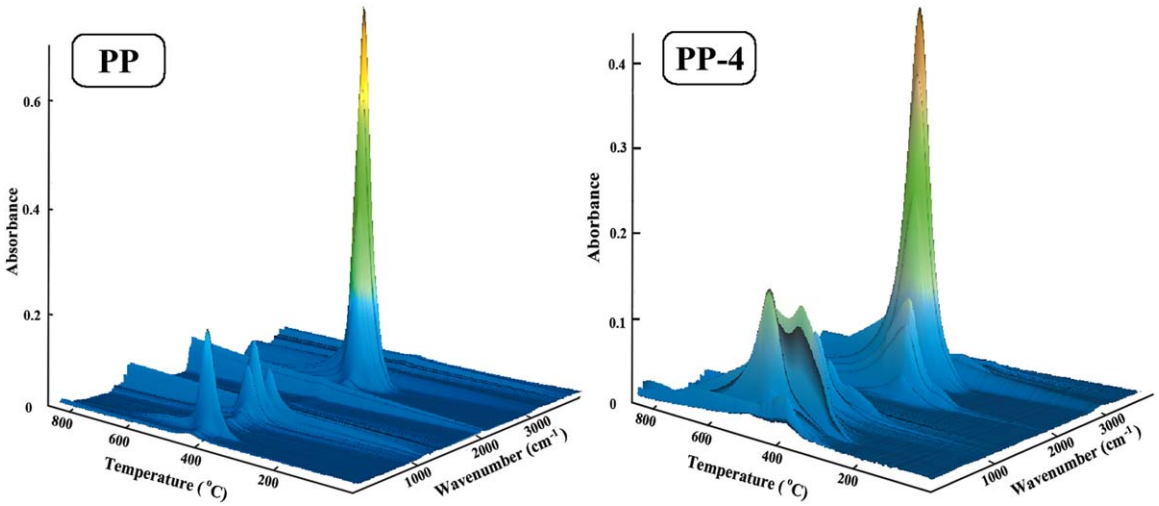


**Figure 10.** 3D TG-FTIR spectra of pyrolysis products during the thermal degradation of PP and PP-4. [Color figure can be viewed in the online issue, which is available at wileyonlinelibrary.com.]

610°C, the experimental result had lower thermostability than the calculated one, indicating that a crosslinking and charring reaction occurred between APP and Si-MCA.[21] Above 610°C, the experimental curve exhibited much higher thermostability, and its residue char at 700°C was as high as 52.3 wt %, whereas it was 31.4 wt % based on the calculation. It was possible to infer that APP could react with Si-MCA and form a thermostable char layer at the high temperature.

Figure 9 presents the FTIR spectra of APP/Si-MCA after heat treatment at different temperatures for 15 min. As can be seen, the relative intensities of the characteristic bands for the APP/Si-MCA mixture were almost unchanged below 250°C. By heating above 300°C, the bands at 3250–3700 $cm^{-1}$ ($\nu_{N-H}$ and $\nu_{O-H}$) became gradually weaker, which could be ascribed to the release of $NH_3$ and $H_2O$ dehydrated by the APP/Si-MCA mixture. Above 400°C, the absorptions in the region 500–2000 $cm^{-1}$ decreased quickly and almost vanished. However, it was worth nothing that the absorptions at 1485 $cm^{-1}$ ($\nu_{-C=N-}$), 1250 $cm^{-1}$ ($\nu_{P-O-C}$), 1030 $cm^{-1}$ ($\nu_{P-O-Si}$), and 799 $cm^{-1}$ ($\nu_{tr.}$) remained and could be still observed even at 650°C, indicating that the dehydration and crosslinking reactions dominated the char-forming process, and the triazine rings were probably crosslinked by —P—O—C— and —P—O—Si— bonds to form the thermostable graphite-like char.[21]

To further clarify the flame retardant mechanism of APP/Si-MCA, TG-FTIR was used to analyze the gas products evolved during the thermal degradation. Figure 10 shows the 3D TG-FTIR spectra of pyrolysis products during the thermal degradation of PP and PP-4. The characteristic spectra obtained at different temperature are presented in Figure 11. For PP, it was hard to observe the infrared absorption signal below 350°C, indicating no decomposition of PP occurred. After that, the infrared absorption peaks at about 2966 $cm^{-1}$, 1645 $cm^{-1}$,

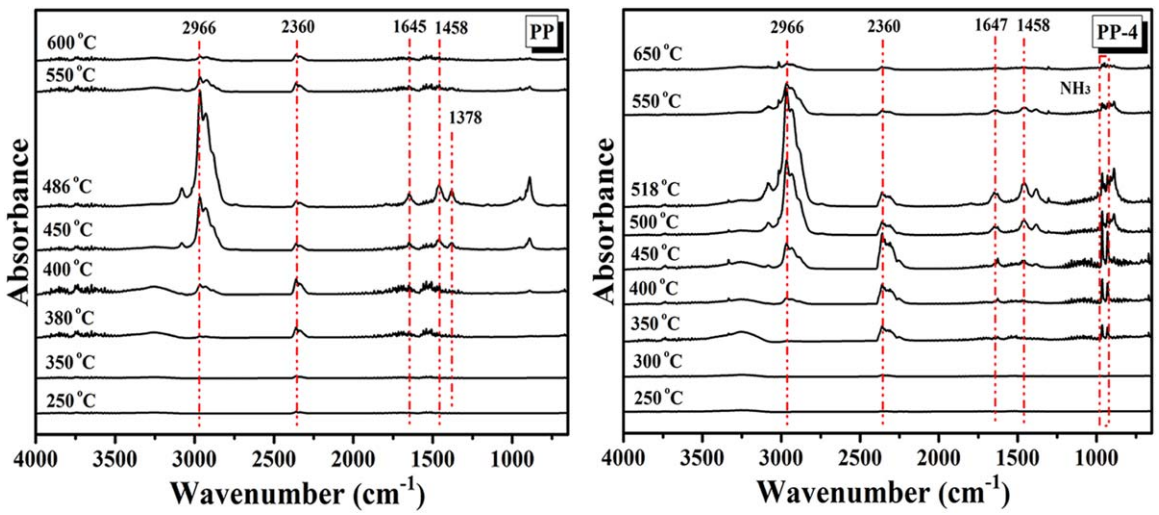


**Figure 11.** FTIR spectra of pyrolysis products of PP and PP-4 at different temperatures. [Color figure can be viewed in the online issue, which is available at wileyonlinelibrary.com.]

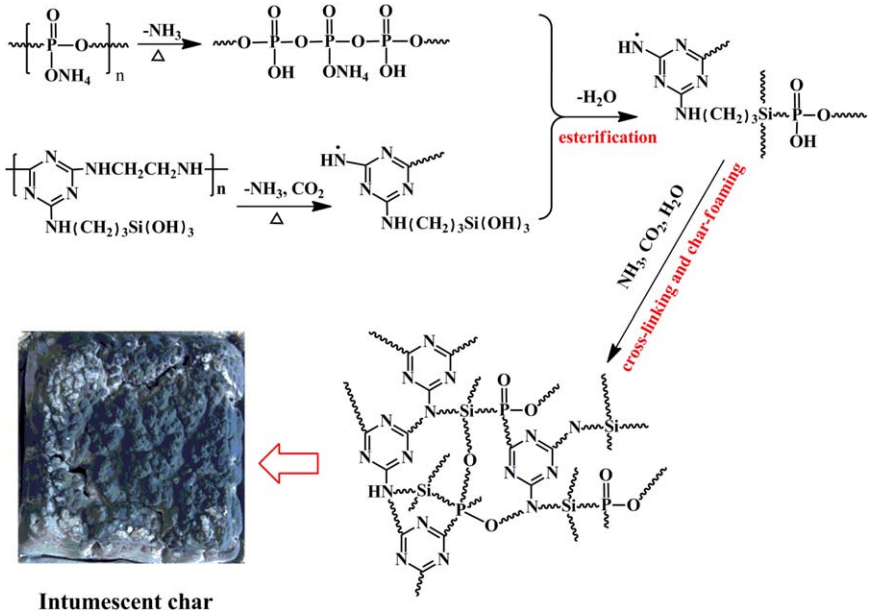


**Figure 12.** Possible flame-retardant mechanism of APP/Si-MCA. [Color figure can be viewed in the online issue, which is available at wileyonlinelibrary.com.]

1458 $cm^{-1}$, and 1378 $cm^{-1}$ were detected, which were attributed to the alkanes, alkenes, and dienes decomposed by PP.[27] With the temperature further increasing, the relative intensity of the absorption peaks increased, resulting from the increasing amounts of pyrolysis gases. Above 550°C, almost all the characteristic peaks decreased quickly and nearly disappeared, indicating that PP was decomposed completely. Compared with PP, the thermal decomposition of the PP-4 was much more complicated. As shown in Figure 11(b), PP-4 started to decompose at 350°C, and the initial volatiles were mainly the incombustible gases, such as $H_2O$ (3400–4000 $cm^{-1}$), $CO_2$ (2340–2370 $cm^{-1}$), and $NH_3$ (930–960 $cm^{-1}$), and so on, which were the products of the esterification of APP/Si-MCA and the decomposition of amino groups.[28] Accordingly, a precursor of intumescent char was formed. Afterward, the alkanes, alkenes, and dienes decomposed by PP were also detected. The maximum signal intensity around 2900 $cm^{-1}$ appeared at about 518°C, which was 32°C higher than that of PP, indicating that APP/Si-MCA could effectively improve the thermostability of PP. These could be explained by that, with increasing temperature, a swollen char was formed and prevented the polymer from decomposing.[29,30] Afterward, the signal intensity of the pyrolysis products decreased gradually, indicating that the decomposition rate of the composite was slowed down by the promoted char formation.

### Possible Flame Retardant Mechanism

Based on the analysis of SEM-EDXS, TGA, FTIR, and TG-FTIR, the possible flame retardant mechanism of APP/Si-MCA is shown in Figure 12. When the temperature was higher than 300°C, APP could release phosphoric acid which catalyze the esterification of the Si—OH of Si—MCA, and formed a precursor of intumescent char (—P—O—Si—).[31] After that, lots of incombustible gases ($NH_3$, $H_2O$, and $CO_2$) were released and swelled the precursor char. As a result, a multicellular swollen char was formed and covered on the polymer. The residue char was rather compact and continuous. With the temperature further increasing, the char did not release flammable gas and maintained excellent thermostability, which could effectively slow down the heat and mass transfer, thus protected the substrate material from burning.

## CONCLUSIONS

An efficient Si-MCA was synthesized successfully, and it showed an excellent synergism with APP in flame retardant PP. The flame retardancy of PP with APP/Si-MCA was improved significantly. When the content of APP was 18.7 wt % and Si-MCA was 6.3 wt %, the LOI value of the composite was 33.5% and the UL 94 test reached a V-0 rating. Meanwhile, the pHRR, THR, av-MLR, and TSP were also decreased greatly. The content of APP/Si-MCA could be reduced to 20.0 wt % to maintain a LOI value of 30.5% and a UL 94 V-0 rating. Moreover, the PP/APP/Si-MCA composite exhibited an outstanding water resistance. After soaking in 70°C water for 168 h, the PP/APP/Si-MCA composite could still obtain a UL 94 V-0 rating at 20.0 wt % IFR loading, whereas the PP/APP/PER composite failed to pass the UL 94 test even at 25 wt % IFR loading. TGA, TG-FTIR, and SEM-EDXS results revealed that there were reactions between the decomposed products of APP and Si-MCA. Meanwhile, a compact and thermostable intumescent char was formed by APP/Si-MCA during the combustion, slowing down the heat and mass transfer, thus effectively protected the polymer from burning.

## ACKNOWLEDGMENTS

We gratefully acknowledge the financial supports by the Guangdong Natural Science Foundation (S2013040015249), the China

Postdoctoral Science Foundation (2014M560660), and the Fundamental Research Funds for the Central Universities (2013ZB0007).

## REFERENCES


1. Bourbigot, S.; Bras, M. L.; Duquesne, S.; Rochery, M. *Macromol. Mater. Eng.* **2004**, *289*, 499.
2. Chen, L.; Wang, Y. Z. *Polym. Adv. Technol.* **2010**, *21*, 1.
3. Wang, J. J.; Wang, L.; Xiao, A. G. *Polym. Plast. Technol. Eng.* **2009**, *48*, 297.
4. Liu, M. F.; Liu, Y.; Wang, Q. *Macromol. Mater. Eng.* **2007**, *292*, 206.
5. Chen, Y. H.; Liu, Y.; Wang, Q.; Yin, H.; Aelmans, N.; Kierkels, R. *Polym. Degrad. Stabil.* **2003**, *81*, 215.
6. Kong, Q. F.; Wang, Z. Z.; Hu, S. X. *Polym. Plast. Technol. Eng.* **2012**, *51*, 1018.
7. Yang, B.; Liu, H.; He, B. B.; Leng, J. H.; Chen, X. *Polym. Compos.* **2013**, *34*, 634.
8. Bras, M. L.; Bourbigot, S.; Felix, E.; Pouille, F.; Siat, C.; Traisnel, M. *Polymer* **2000**, *41*, 5283.
9. Liu, Y.; Yi, J. S.; Cai, X. F. *J. Therm. Anal. Calorim.* **2011**, *107*, 1191.
10. Yi, J. S.; Liu, Y.; Pan, D. D.; Cai, X. F. *J. Appl. Polym. Sci.* **2013**, *127*, 1061.
11. Chen, J.; Liu, S. M.; Zhao, J. Q. *Polym. Degrad. Stabil.* **2011**, *96*, 1508.
12. Jiang, W. Z.; Hao, J. W.; Han, Z. D. *Polym. Degrad. Stabil.* **2012**, *97*, 632.
13. Tian, N. N.; Wen, X.; Gong, J.; Ma, L.; Xue, J.; Tang, T. *Polym. Adv. Technol.* **2013**, *24*, 653.
14. Hu, X. P.; Li, Y. L.; Wang, Y. Z. *Macromol. Mater. Eng.* **2004**, *289*, 208.
15. Li, B.; Xu, M. J. *Polym. Degrad. Stabil.* **2006**, *91*, 1380.
16. Dai, J. F.; Li, B. *J. Appl. Polym. Sci.* **2010**, *116*, 2157.
17. Yang, K.; Xu, M. J.; Li, B. *Polym. Degrad. Stabil.* **2013**, *98*, 1397.
18. Feng, C. M.; Zhang, Y.; Liu, S. W.; Chi, Z. G.; Xu, J. R. *J. Appl. Polym. Sci.* **2012**, *123*, 3208.
19. Feng, C. M.; Zhang, Y.; Liu, D.; Liu, S. W.; Chi, Z. G.; Xu, J. R. *J. Anal. Appl. Pyrol.* **2013**, *104*, 59.
20. Chen, X. L.; Jiao, C. M. *Polym. Adv. Technol.* **2011**, *22*, 817.
21. Lai, X. J.; Zeng, X. R.; Li, H. Q.; Liao, F.; Yin, C. Y.; Zhang, H. L. *Polym. Compos.* **2012**, *33*, 35.
22. Hamdani, S.; Longuet, C.; Perrin, D.; Lopez-Cuesta, J. M.; Ganachaud, F. *Polym. Degrad. Stabil.* **2009**, *94*, 465.
23. Chen, X. L.; Jiao, C. M. *J. Polym. Res.* **2009**, *16*, 537.
24. Ye, L.; Wu, Q. H.; Qu, B. J. *J. Appl. Polym. Sci.* **2010**, *115*, 3508.
25. Wang, H. F.; Li, B. *Polym. Adv. Technol.* **2010**, *21*, 691.
26. Zhou, R. M.; Lai, X. J.; Li, H. Q.; Tang, S.; Zeng, X. R. *Polym. Compos.* **2014**, *35*, 158.
27. Zhang, F.; Zhang, J.; Sun, D. X. *J. Thermoplast. Compos.* **2009**, *22*, 681.
28. Wu, K.; Hu, Y.; Song, L.; Lu, H. D.; Wang, Z. Z. *Ind. Eng. Chem. Res.* **2009**, *48*, 3150.
29. Wu, K.; Kandola, B. K.; Kandare, E.; Hu, Y. *Polym. Compos.* **2011**, *32*, 378.
30. Wu, N.; Yang, R. J. *Polym. Adv. Technol.* **2011**, *22*, 495.
31. Xu, Z. Z.; Huang, J. Q.; Chen, M. J.; Tan, Y.; Wang, Y. Z. *Polym. Degrad. Stabil.* **2013**, *98*, 2011.